Feasibility study for thermal-field directed self-assembly of heteroepitaxial quantum dots

Lawrence H. Friedman and Jian Xu
Department of Engineering Science and Mechanics, Pennsylvania State University, 212 Earth and Engineering Science Building, University Park, Pennsylvania 16802

(Received 25 October 2005; accepted 17 January 2006; published online 27 February 2006)

Strain mismatched semiconductors are used to form self-assembled quantum dots (SAQDs). An important step in developing SAQD technology is to control randomness and disorder in SAQD arrays. There is usually both spatial and size disorder. Here, it is proposed to use spatially varying heating as a method of to direct self-assembly and create more ordered SAQD arrays or to control placement of single dots or dot clusters. The feasibility of this approach is demonstrated using a 2D computational model of Ge dots grown in Si based on finite element analysis of surface diffusion and linear elasticity. © *2006 American Institute of Physics*. [DOI: 10.1063/1.2179109]

Self-assembly of quantum dots represents an important step in the advancement of semiconductor fabrication at the nanoscale that will allow breakthroughs in electronics and optoelectronics. The two most studied systems are Ge_xSi_{1-x} dots grown on a Si substrate and $In_xGa_{1-x}As$ dots grown on a GaAs substrate. The former being most interesting for electronic applications and possibly even optoelectronic applications, and the latter being most useful for optoelectronic applications. An important step in developing self-assembled quantum dots (SAQD) technology is to control randomness and disorder in SAQD arrays.

Two types of disorder arise in SAQDs, size disorder, where dots of varying sizes form, and spatial disorder, where the dots form an essentially random arrangement on a substrate. The mentioned SAQD systems and others would become much more useful if one could either (a) generate large arrays of regularly spaced and/or regularly sized SAQDs or (b) be able to place SAQDs in desired locations. Controlling self-assembly in such a fashion to produce this outcome is known as "directed self-assembly."

Directed self-assembly is possible because SAQD formation takes place on a nominally flat and homogeneous substrate. The energy landscape of SAQD configurations is highly degenerate, meaning that there is no strong reason to choose one arrangement over another. Thus, SAQDs nucleation and growth is directed by random low-amplitude noise such as thermal fluctuations and crystal imperfections. The key to directed self-assembly is to provide a signal that preferentially selects a desirable final state of the growing system. Three examples of how the random noise can be overcome are demonstrated by the preferential nucleation of SAQDs above intersection points of an array of misfit dislocations,[1] nucleation of quantum dots on etched mesas,[2] and the ability to nucleate SAQD clusters using a focused ion beam (FIB).[3]

Here, thermal-field directed self-assembly is proposed whereby spatially varying heating is used to influence the formation and evolution of SAQDs. One can imagine various methods to accomplish this. For example, a laser interference pattern has been used to direct the self-assembly of metal clusters on a Si substrate.[4] One might also try low energy ion bombardment or heating with an electron beam. The feasibility of using spatially varying heating with proper growth conditions to enhance order of SAQDs is demonstrated using a 2D computational model of Ge dots grown on Si. One can use an interference pattern such as in Refs. 4 and 5 to produce an array with greatly enhanced spatial and size ordering, or one can use a focused hot spot to produce a quantum dot cluster (similar to a quantum fortress[6]) or even a single dot. This proposal is justified through computational experiment using a 2D numerical model of elasticity and surface diffusion.

The model description is broken into two parts. First, the physical and mathematical model is presented. Then the numerical implementation using FEMLAB is discussed.

The growing film evolves due to surface diffusion that is driven by a chemical potential μ. The model is implemented in two dimensions with a 1D evolving surface (Fig. 1). It is similar to Ref. 7, except that the surface energy is isotropic and not a function of the orientation. At any instant in time, the growing film is described by the curve $y=h(x)$. The surface grows with a velocity normal to the surface,

$$v_n = n_y \frac{dh}{dt} = \nabla_S \cdot \mathcal{D} \nabla_S \mu + n_y Q, \tag{1}$$

where ∇_S is the surface gradient, $\nabla_S \cdot$ is the surface divergence, $\mathcal{D}$ is the surface diffusion constant, n_y is the y-component of the surface normal $\hat{n}$, and Q is the flux of new material onto the surface,

$$\mathcal{D} = \frac{D_S c_S}{k_b T} \exp\left[-\frac{\Delta E}{k_b T} \right], \tag{2}$$

where D_S is the intrinsic surface diffusivity, c_S is the mobile surface atoms per unit area, and ΔE is the surface diffusion activation energy. The diffusion potential is

$$\mu = \Omega \left(\omega - \kappa(\gamma + W) + n_y \frac{dW}{dy} \right) \tag{3}$$

where Ω is the atomic volume, ω is the strain energy density at the free surface, $\kappa = \mathrm{Tr}(\nabla_S \hat{n})$ is the total surface curvature, γ is the surface energy density, and W is the wetting potential that is a function of the film height y. The strain energy ω is found using isotropic linear plane strain elasticity. In general, ω is a function of x, and it is a nonlocal functional of the entire surface profile $h(x)$.

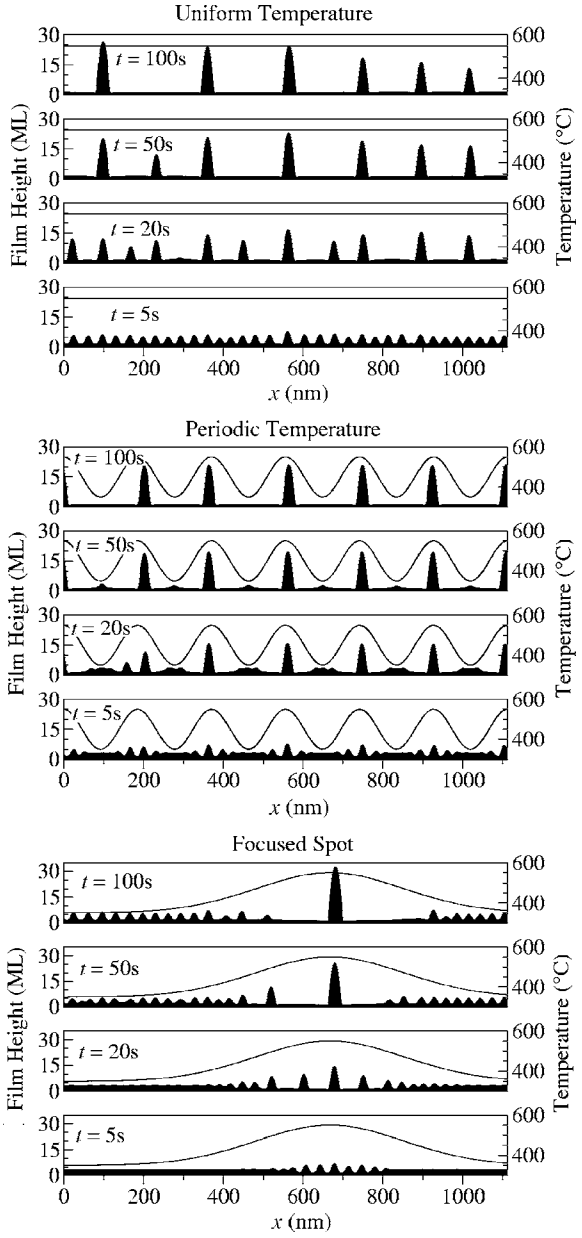

FIG. 1. *Simulation results*: Solid line (—) indicates temperature profile. Filled pattern indicates film height. The graphs are not to scale as the dot aspect ratios are stretched in the vertical direction for clarity.

The source of heating is not specifically modeled. It is *assumed* that one can create a spatially varying temperature profile with a temperature difference $\Delta T=200\ ^\circ\mathrm{C}$ and a characteristic wavelength as small as $\lambda=150$ nm. From Eq. (2), high temperatures will enhance diffusion, while low temperatures will suppress surface diffusion.

The model is implemented numerically with FEMLAB, a Finite Element Analysis Package.[8] FEMLAB does not directly support moving boundaries, so the elasticity part of the problem is solved using a time-dependent coordinate transformation. Real space is represented by the variables x and y, while the mesh lies in the dimensionless ξ-η space. The method is similar to the method of parametric elements. In real space the substrate/film have a width w_i and a height h_i ($i=s$ for substrate or f for film). In calculation space, the substrate/film mesh has a width $l_{x,i}$ and height $l_{y,i}$. Thus, within the film or substrate,

$$x=\frac{w}{l_x}(\xi-\xi_0)+x_0, \tag{4}$$

$$y=\frac{h(\xi)}{l_y}(\eta-\eta_0)+y_0. \tag{5}$$

$h(\xi)$ is a spatially varying function for the film, but for the substrate, it is a constant, $h(\xi)\rightarrow h_s$. In real space (x-y plane), the conserved flux quantity is stress, $\tilde{\sigma}$, so that $\nabla\cdot\tilde{\sigma}=0$ where

$$\tilde{\sigma}=\tilde{E}:\left[\frac{\partial \boldsymbol{u}}{\partial \boldsymbol{x}}\right]_{\text{symmetric}}, \tag{6}$$

and $\tilde{E}$ is the four-dimensional linear elasticity stiffness tensor. In calculation space (ξ-η plane), the conserved flux quantity is

$$\tilde{\Gamma}=(\det\tilde{\Lambda})\tilde{\Lambda}^{-1}\cdot\tilde{E}:\left[\tilde{\Lambda}^{-1}\cdot\frac{\partial \boldsymbol{u}}{\partial \boldsymbol{\xi}}\right]_{\text{symmetric}}$$

so that $\nabla\cdot\tilde{\Gamma}=0$, where $\tilde{\Lambda}=\partial \boldsymbol{x}/\partial \boldsymbol{\xi}$ is the Jacobian matrix. Plane-strain elasticity is used because it will give the appropriate linear behavior when ripple-patterned growth instabilities first set in (see Ref. 9). Periodic boundary conditions are implemented to minimize the effects of the simulation's finite size.

Ideally, the surface velocity equation (1) should be modified to include a noise term; however, such a term would complicate the simulation and would be nearly impossible to implement in FEMLAB. Thus, noise $[\chi(x)]$ is incorporated into the initial conditions only, $h_0\rightarrow h_0+\chi(x)$.

Physically meaningful and dimensionful values are chosen for all simulation parameters to demonstrate the plausibility of the proposed mechanisms to direct self-assembly. For Ge dots grown on Si, as given in Ref. 9, the Young moduli are $E_{\mathrm{Ge}}=1.361\times10^{12}\ \mathrm{dyn/cm^2}$ and $E_{\mathrm{Si}}=1.660\times10^{12}\ \mathrm{dyn/cm^2}$, the Poisson ratios are $\nu_{\mathrm{Ge}}=0.198$ and $\nu_{\mathrm{Si}}=0.217$, the mismatch strain is $\epsilon_0=-0.0418$, the atomic volume is $\Omega=2.27\times10^{-23}\ \mathrm{cm^3}$, the surface energy density is $1927\ \mathrm{erg/cm^2}$, the intrinsic diffusivity is $D_S=8.45\times10^{-6}\ \mathrm{cm^2/s}$, the surface concentration is $c_S=1.25\times10^{15}\ \mathrm{cm^{-2}}$, and the activation energy is $\Delta E=1.33\times10^{-12}$ erg. The wetting potential $W(h)=(7.59\times10^{-7}\ \mathrm{erg/cm^2})/h$. Combined with the stabilizing effect of the substrate stiffness,[9] $W(h)$ stabilizes planar growth until $h\approx2.75$ ML$=7.47$ Å.

Three growth processes are simulated and reported on. *Simulation 1* is the control simulation. At a spatially uniform temperature of $T=550\ ^\circ\mathrm{C}$, a film is grown beyond the wetting layer height and then allowed to relax, resulting in island formation and ripening. The next two simulations are identical to the first except that they have temperature profiles ranging from $T_{\mathrm{low}}=350\ ^\circ\mathrm{C}$ to $T_{\mathrm{high}}=550\ ^\circ\mathrm{C}$. For *Simulation 2* a spatially periodic temperature profile of periodicity $\lambda=185$ nm is used, resulting in enhanced space and size ordering after some ripening. *Simulation 3* models growth and annealing in the presence of a hot spot of width 371 nm that results in a patch of SAQDs that finally ripens into one large central dot.

Other than the temperature profile, the details of each simulation are the same. Each simulation is carried out on a periodic simulation cell of width $w=1.112\ \mu$m and a substrate height of $h_s=1.112\ \mu$m. The initial film height is al-

ways $h_0=2.75$ ML$=7.47$ Å with a noise amplitude of 1 Å. This height is just above the threshold for nonplanar film growth. With their respective temperature profiles, films are then grown a little more at a rate of 0.25 ML/s$=0.68$ Å/s for 2 s. The films are then annealed for the remainder of the simulation using the respective temperature profile.

The result of each simulation is shown in Fig. 1. The effect of the spatially varying temperature profile in *simulations* 2 and 3 is that SAQDs form and evolve more quickly at the temperature peaks due to the enhanced diffusivity in hotter regions. During ripening ($t>2$ s), this head start becomes an advantage for dots near the temperature peaks as they grow at the expense of their smaller less mature neighbors. The end result at $t=100$ s is that relatively large dots remain at or near temperature peaks while their neighbors have been absorbed. In *simulation* 3, distant cold ($T=350\ ^\circ$C) regions contain small dots similar to the initial dots at $t=5$ s. Compared to the control (*simulation* 1), the periodic temperature profile produces enhanced spatial and size ordering, while the simulated hot spot (*simulation* 3) shows that after sufficient ripening, an isolated dot forms near a temperature peak.

These simulated experiments are optimistic in the sense that it is assumed one can create hot spots on the order of 150–300 nm. This size range is achievable via UV lasers such as organic dye lasers or excimer lasers, as the power wavelength is half the amplitude wavelength. Smaller hot spots achieve higher quantum dot density and better placement precision. This trend is probably limited by the initial SAQD size or critical wavelength discussed in Ref. 9. Here, the simulated temperature profile ($\lambda>150$ nm) is much larger than the initial dot size (30 nm by inspection).

Ideally, one would like to use a 3D computational model (with a 2D surface), but this work represents an initial study and more sophisticated modeling will follow. In addition to 3D modeling, other enhancements should include orientation dependent surface energy as in Ref. 7, elastic anisotropy, and specific modeling of heating, heat flow, and thermal expansion.

Thermal-field directed self-assembly of quantum dots represents an exciting possibility. For example, in addition to enhanced ordering, one might be able to write structures by sweeping a beam (laser or perhaps electron). Of course, these simulations only show the most basic potential, but clearly the possibilities warrant further investigation.

[1] S. Yu Shiryaev, E. Verstlund Pedersen, F. Jensen, J. Wulff Petersen, J. Lundsgaard Hansen, and A. Nylandsted Larson, Thin Solid Films **294**, 311 (1997).
[2] S. Krishna, D. Zhu, J. Xu, and P. Bhattacharya, J. Appl. Phys. **86**, 6135 (1999).
[3] R. Hull, J. L. Gray, M. Kammler, T. Vandervelde, T. Kobayashi, P. Kumar, T. Pernell, J. C. Bean, J. A. Floro, and F. M. Ross, Mater. Sci. Eng., B **101**, 1 (2003).
[4] Chi Zhang, Wei Zhang, Adam Bauer, and Ramki Kalyanaraman, in TMS Annual Meeting 2005, San Francisco, February, 2004, TMS, p. 21.
[5] C. Zhang and Ramki Kalyanaraman, J. Mater. Res. **19**, 595 (2004).
[6] Thomas E. Vandervelde, Piyush Kumar, Takeshi Kobayashi, Jennifer L. Gray, Tim Pernell, Jerrold A. Floro, and John C. Bean, Appl. Phys. Lett. **83**, 5205 (2003).
[7] Y. W. Zhang and A. F. Bower, Appl. Phys. Lett. **78**, 2706 (2001).
[8] FEMLAB version 3.1i (COMSOL AB, Stockholm, 2005).
[9] B. J. Spencer, P. W. Voorhees, and S. H. Davis, J. Appl. Phys. **73**, 4955 (1993).